Green synthesis of chitosan-based nanofibers and their applications†

Lei Qian and Haifei Zhang*

Received 23rd December 2009, Accepted 21st April 2010
First published as an Advance Article on the web 18th May 2010
DOI: 10.1039/b927125b

We report here a simple and green method for the preparation of chitosan and chitosan-based nanofibers by freeze-drying dilute aqueous solutions, without the use of organic solvent, high concentration of acid solutions, or the need to pre-treat chitosan. Chitosan nanofibers with diameters ranging from 100 to 700 nm were obtained from aqueous chitosan solutions with the concentrations equal to or below 0.1 wt %. Chitosan/poly(vinyl alcohol) blend nanofibers with different mass ratios were produced by freeze-drying the mixture solutions. The effects of solution concentration, chitosan molecular weight, and freezing temperature were examined. The morphology and thermal stability of the nanofibers were analyzed. Pore size and pore volume of the bulk fibrous materials were measured. A uniform coating of calcium phosphate was formed on the chitosan nanofibers in a 5 times concentrated simulated body fluid. The adsorption of copper ions by chitosan nanofibers from aqueous solutions was investigated. It was found that chitosan nanofibers exhibited a high adsorption capacity of Cu^{2+} at 2.57 mmol g^{-1} of chitosan for aqueous $CuSO_4$ solution at a concentration of 1000 ppm. Loading and release of small molecules (Rhodamine B) and protein molecules (bovine serum albumin) with chitosan nanofibers as scaffolds were also investigated.

1. Introduction

Chitosan is the deacetylated derivative of chitin which is the second most abundant polysaccharide found in crab, shrimp shells, and fungal mycelia. Chitosan is a polycationic polymer with a large amount of primary amines showing useful properties including biocompatibility, biodegradability, adsorption activity, and antimicrobial ability.[1] Therefore, chitosan has been widely utilized in tissue engineering, drug delivery, filtration, and biosensors.[2] For example, chitosan with a sponge-like structure was incorporated with a platelet-derived growth factor and then used as an osteoconductive material for bone regeneration.[2b] Porous chitosan containing calcium phosphate was employed as a scaffold for controlled antibiotic drug delivery.[2c] Chitosan could bind toxic heavy metal ions such as Zn^{2+}, Cu^{2+}, CrO_4^{2-} and Mg^{2+} from aqueous solutions due to the amine groups on the chitosan backbone.[3]

Polymeric nanofibers mimic the structure and function of natural extracellular matrix (ECM) and can be used as scaffolds for tissue engineering and drug delivery.[4] These fibers are usually produced by electrospinning, phase separation, or self-assembly.[5] Chitosan molecules have a proxy structure of glycosaminoglycan, an important component of the native ECM to enhance cell attachment and proliferation and improve the cellular and tissue biocompatibility.[6] Therefore, the preparation of chitosan nanofibers has been extensively investigated for various applications. However, the production of chitosan nanofibers is still a challenge although electrospinning has been widely used to prepare polymer fibers. Chitosan shows high crystallinity and high degree of hydrogen bonding. This leads to poor solubility in water and common organic solvents. To form fibers by electrospinning, the polymer concentration needs to be at least 2 to 2.5 times the entanglement concentration.[7] However, chitosan solutions at these concentrations are highly viscous and can be very difficult for an electrospinning process.

In order to obtain chitosan nanofibers *via* electrospinning, different preparation procedures have been used including mixing with other polymer solutions, adding organic solvents as co-solvents, or using highly concentrated acetic acid solution.[8] In the mixing method, polyethylene oxide and poly(vinyl alcohol) (PVA) are often used to blend with chitosan solutions. The blending mass ratio is an important factor for the formation of the nanofibers. For example, the fiber structure was only formed by electrospinning when the chitosan/PVA mass ratio was lower than 1.[8e] Tri-fluoroacetic acid, hexafluoro-2-propanol and dichloromethane were added to prepare chitosan nanofibers by electrospinning.[8f,g] The toxicity and high cost associated with these organic solvents limited their applications. Chitosan nanofibers could be obtained with the use of concentrated aqueous acetic acid solution (acid content 90%).[8h] Although the concentration of acetic acid could be reduced to 70% after hydrolyzing chitosan solutions for 48 h before electrospinning,[8i] the high concentration of acid was still highly corrosive. Because of the limitation and disadvantage of the above-mentioned methods, it is necessary and also very important to find a simple and green method for the production of chitosan nanofibers.

Freeze-drying is a process widely used to prepare porous materials as scaffolds for tissue engineering. The process

Department of Chemistry, University of Liverpool, Crown Street, Liverpool, United Kingdom L69 7ZD. E-mail: zhanghf@liv.ac.uk; Fax: +44 151 7943588

† Electronic supplementary information (ESI) available: Characterisation of chitosan nanofibers. See DOI: 10.1039/b927125b

normally includes two steps: (1) freeze a solution in a cold bath and (2) freeze-dry the frozen sample under vacuum to remove the solvent by sublimation. Without using an organic solvent, freeze-drying is potentially a green route to prepare porous materials. Freeze-drying aqueous polymer solutions normally results in porous structures with different pore morphologies.[9] In a recent communication, we reported the preparation of polymeric nanofibers by freeze-drying dilute polymer solutions of sodium carboxymethyl cellulose, sodium alginate, and PVA.[10] These polymer nanofibers are soluble in water, which limits their potential applications as support for controlled delivery and tissue engineering. Here, we describe the preparation of chitosan and chitosan-based nanofibers *via* the freeze-drying route. The diameter of the nanofibers is in the range of 100 nm to 700 nm. These nanofibers are not soluble in water at pH>6.5. The pH of the dilute chitosan solution at a concentration of 0.1 wt% was about 4.0, which was only slightly corrosive.[8] Indeed, there was no problems found when freeze-drying aqueous chitosan solutions in this study. To show the versatility of this method, chitosan/PVA blend nanofibers with different mass ratios were produced. The chitosan nanofibers were further modified with a coating layer of calcium phosphate by employing a biomimetic mineralization process in a 5 times concentrated simulated body fluid (SBF). The chitosan nanofibers were then assessed for adsorption of Cu^{2+} ions in water and as scaffolds for the release of Rhodamine B and bovine serum albumin.

2. Experimental

2.1 Chemicals and reagents

Chitosan with low molecular weight (deacetylation 75-85%, Mw 50-190 KDa), medium molecular weight (deacetylation 75-80%, Mw 190–310 KDa) and high molecular weight (deacetylation > 75%, approximately 310 KDa – >375 KDa); poly(vinyl alcohol) (PVA, 99+% hydrolyzed, Mw 89–98 KDa) were used as received from Aldrich. Bovine serum albumin (BSA, *cohn V fraction*) was obtained from Sigma. Rhodamine B (RhB) was purchased from ACROS. Acetic acid (99%), NaCl, KCl, $CaCl_2$, $MgCl_2{\cdot}6H_2O$, NaH_2PO_4, $NaHCO_3$ were obtained from BDH. 5 times concentrated SBF solutions (5-SBF) were prepared according to the reported method.[11] Briefly, a stock solution containing 1 M NaCl, 5 mM KCl, 25 mM $CaCl_2$, 5 mM $MgCl_2$, 10 mM NaH_2PO_4 was firstly prepared and 4.2 mg $NaHCO_3$ was added into 10 ml 5-SBF under vigorous stirring just before starting the mineralization process. $CuSO_4{\cdot}5H_2O$ was purchased from Fisher Scientific. The phosphate buffer solution (PBS) for the BSA release was prepared by mixing 20 ml 0.2 M K_2HPO_4 and 11.85 ml 0.2 M NaOH and then diluting the solution to 80 ml with distilled water. Distilled water was used to prepare all aqueous solutions.

2.2 Preparation of chitosan and chitosan-based nanofibers

Aqueous chitosan solutions (1 wt%) with different molecular weights were prepared by dissolving 0.2 g chitosan into 20 ml water containing 120 µl acetic acid. The 1 wt% chitosan solution was diluted to 0.5, 0.1, 0.05 and 0.02 wt% for the freezing process. The pH for 0.1 wt% chitosan solution was determined to be 4. The diluted chitosan solutions were frozen in liquid nitrogen or in a freezer (–20 °C) and then freeze-dried in a freeze-dryer (Vis Advantage) at the shelf temperature of –10 °C for 48 h. All the solutions were frozen in liquid nitrogen unless otherwise stated. For chitosan/PVA blend nanofibers, 0.1 wt% chitosan solutions were mixed with 0.1 wt% PVA with different volume ratios before freezing in liquid nitrogen. The chitosan solutions containing RhB or BSA at concentrations of 4.95 µg RhB/ml 0.1 wt% chitosan, 0.36 µg RhB/ml 0.1 wt% chitosan, 1.80 µg RhB/ml 0.5 wt% chitosan, 3.60 µg RhB/ml 1.0 wt% chitosan, 1.0 mg BSA/ml 0.1 wt% chitosan, and 0.5 mg BSA/ml 0.1 wt% chitosan were frozen in liquid nitrogen and then freeze dried to produce the scaffolds for the controlled release.

2.3 Swelling property of chitosan nanofibers

Chitosan structures prepared from 0.1, 0.5 and 1.0 wt% solutions were soaked in ethanol for 30 min and then filtered and dried in a vacuum oven. This was performed to remove the residual acetic acid in the materials. The dry structures were soaked in water for different time intervals and then taken out. After removing excess water on the surface, the chitosan materials were weighed immediately. The swelling capability was assessed by the swelling ratio:

$$\text{Swelling ratio} = (W_2 - W_1)/W_1$$

W_1 is the mass before soaking in water; W_2 is the mass after soaking in water for different time intervals.

2.4 Mineralization on chitosan nanofibers

1.5 mg chitosan nanofibers was immersed into 10 ml 5-SBF. The solution was replaced with fresh 5-SBF every 2 h. After 6 h, chitosan nanofibers were removed from the 5-SBF, gently washed with water and then dried in air at room temperature.

2.5 Chitosan nanofibers for Cu^{2+} adsorption

Chitosan nanofibers were firstly washed with ethanol and dried in a vacuum oven. The dry chitosan nanofibers (4.0 mg) were immersed into a $CuSO_4$ solution (12.0 ml) with the concentration ranging from 50 to 1000 ppm while stirring for 16 h. After that, the composite nanofibers were taken out. The adsorption capacity was calculated from measurement of Cu^{2+} concentration in the aqueous solution before and after adsorption. Measurements were performed in triplicate and the average value was obtained.

2.6 Controlled release from chitosan scaffolds

5.5 mg chitosan material containing different amount of RhB or BSA was immersed into a 2.5 ml PBS (pH 7.0). At different release times, 200 µl buffer solution was taken out and used to determine the concentration of RhB or BSA by UV-Vis spectroscopy. 200 µl fresh PBS was added back to maintain the volume. The standard curves were obtained by measuring absorbance of solutions prepared with known concentrations of RhB (0.09–18.0 µg ml^{-1}) and BSA (0.025–10.0 mg ml^{-1}). Triplicate tests were carried out for each releasing condition. The maximum absorbance at 550 nm for RhB and 280 nm for BSA were used to obtain the concentrations after releasing into PBS. The cumulative released amount at a releasing time t was calculated based on the equation below:

$$Q_t = C_n V_t + \sum C_{n-1} V_s$$

Where C_n is the concentration of RhB or BSA at the releasing time t and the number of samples being taken for the UV analysis is n; V_t is the volume of PBS solution; V_s is the sample volume taken out for the UV detection. The released percentages, $Q_t/Q_\infty \times 100\%$ where Q_∞ is the amount (mol) of RhB or BSA incorporated into the nanofibers, were plotted as a function of time.

2.7 Characterization

Morphology of the prepared materials was examined by a Hitachi-4800 scanning electron microscope (SEM) with an energy dispersive X-ray (EDX) microanalysis detector (INCA 7200, Oxford Instrument). The samples were adhered to SEM studs, and then coated with gold using a sputter-coater (EMITECH K550X) for 3 min at 35 mA. Pore volume and macropore size distribution were obtained using a Micromeritics Autopore IV 9500 porosimeter with a pressure range from 689 pa to 1.308×10^4 kPa. Thermal stability of chitosan nanofibers was assessed using a thermogravimetric analyzer (TGA, TA instruments, Q5000IR). The samples were heated at 10 °C min^{-1} from 50 to 600 °C. Inductively coupled plasma emission spectrometry (ICP-ES) was used to measure the concentration of copper ions in water. The release of RhB and BSA in the solution was monitored by a UV plate reader (μQuant, Bio-Tek instrument Inc.) using an acrylic 96-well plate. The powder X-ray diffraction (PXRD) pattern was obtained using a Panalytical X' Pert Pro diffractometer with Co Kα radiation operated at 40 mA and 40 KV.

3. Results and discussion

3.1 Chitosan nanofibers

Chitosan with medium molecular weight (MMw) was employed to study the effect of concentration on the formation of nanofibers. The morphology of the materials was changed from a macroporous structure to nanofiber structures when the concentration of chitosan solutions was decreased from 1.0 wt% to 0.02 wt% (Fig. 1). The pore structure obtained from 1.0 wt% chitosan solution (Fig. 1a) was similar to the structures prepared from freeze-drying other polymer solutions (≥0.5 wt%).[10] Fibre structure was observed when the concentration was reduced to 0.1 wt%. The diameter of these fibers was in the range of 300 to 700 nm (Fig. 1b), similar to the PVA nanofibers produced in the previous study.[10] When a 0.05 wt% chitosan solution was freeze-dried, a kind of *nanobelt* structure was observed (Fig. 1c), which could be clearly seen from the image at a higher magnification (inset of Fig. 1c). When the concentration of chitosan solution was reduced further to 0.02 wt%, the aligned nanofibers with diameters from 100 to 500 nm were produced (Fig. 1d). The alignment of the fibers was formed due to the rapid freezing process. In principle, it was possible to produce chitosan nanofibers with a high degree of alignment by carefully controlling the freezing condition.[12] These images showed that the concentration of chitosan was very important for the formation of nanofibers. The formation of nanofiber structure could be explained as follows: during the freezing process, ice crystals started to nucleate and grow. The chitosan molecules were excluded and aggregated between ice crystals. Due to the small number of molecules available in the solutions, chitosan molecules formed fibrous structures rather than porous structures after freeze drying. For the solution with a higher concentration, the large amount of chitosan molecules tended to aggregate to form porous structures other than nanoscale fibers.[9] However, different from the other types of polymer nanofibers,[10] the nanobelt structure was observed for chitosan fibers (Fig. 1c). The belt structure could still be observed at lower concentrations when imaging from different angles. However, the belt structure was not so obvious due to the morphology change at 0.02 wt%, *i.e.*, beads also formed on the fibers. This kind of structure was concentration-dependant and might be formed due to the presence of carbonyl and amino groups on chitosan molecules and the π–π interaction between chitosan chains under certain preparation conditions. It was possible that crystalline phases were formed in the chitosan structure.[13] A further detailed study would be required to elucidate the mechanism of the formation of the nanobelt structure.

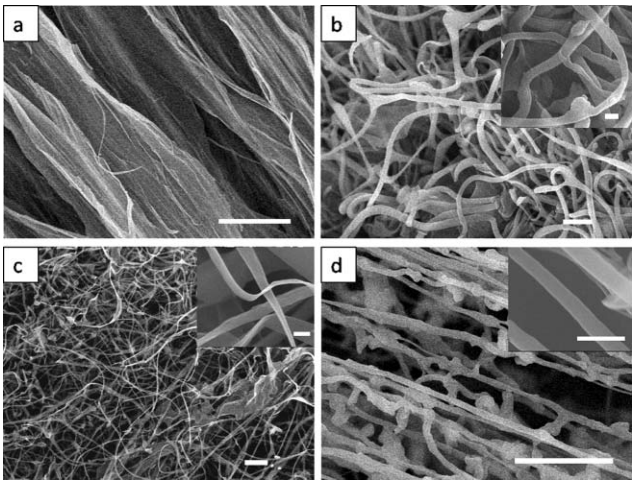

Fig. 1 SEM images of chitosan structures from freeze-drying chitosan (MMw) solutions with different concentrations. (a) 1 wt%, scale bar 50 μm; (b) 0.1 wt%; (c) 0.05 wt%; (d) 0.02 wt%. In (b)–(d), all scale bars 5 μm, inset scale bars 500 nm.

Dilute chitosan solutions with low and high molecular weight (LMw and HMw) were also employed in the freeze-drying process. Chitosan nanofibers were obtained by freeze-drying the aqueous solutions at the concentration of 0.02 wt% (Fig. S1†). This indicated that chitosan nanofibers with different molecular weight could be formed by freeze-drying the dilute aqueous solutions.

The effect of freezing temperature was also investigated. When the 0.1 wt% chitosan (MMw) solution was frozen in liquid nitrogen and then freeze-dried, a nanofiber structure was produced (Fig. 1b). However, when the same solution was frozen in a freezer (–20 °C) and then freeze-dried, a random macroporous structure was obtained (Fig. S2†). Due to the slow freezing rate and low temperature gradient at –20 °C, the freezing process led to the random growth of larger ice crystals and a larger amount of polymer molecules aggregated between the larger ice crystals. A disordered large porous material was thus obtained after removing ice crystals.

The stability of chitosan nanofibers in water was examined. Chitosan nanofibers from freeze-drying the 0.1 wt% chitosan (MMw) solution were washed in ethanol for 30 min and dried in a vacuum oven to remove the residual acetic acid. The chitosan nanofibers were immersed into water to study the stability. The wet material was dried in the vacuum oven at room temperature, weighed, and then placed back into water every week for 10 weeks. No obvious mass change was observed. The fibrous structures retained their shape although the fibers' packing became denser after washing and drying in a vacuum oven. This indicated that the chitosan nanofibers exhibited good stability towards water.

3.2 Chitosan/PVA blend nanofibers

The mixture of chitosan and PVA solutions was freeze-dried to prepare blend nanofibers. The mixture solutions were prepared by mixing these two polymer solutions at a concentration of 0.1 wt% with volume ratios of 9 : 1, 7 : 3, 5 : 5 and 3 : 7. After the freeze-drying process, chitosan/PVA nanofibers with varied compositions were obtained. Fig. 2a and b show the SEM images of chitosan/PVA nanofibers with composition ratios 7 : 3 and 5 : 5. Diameters of these blend nanofibers were 200–600 nm (for ratio 7 : 3) and 200–500 nm (for ratio 5 : 5). The size of the blend nanofiber was smaller than those of chitosan nanofibers made from 0.1 wt% chitosan solutions containing no PVA. Nanofiber structures were also observed for the samples prepared from the mixture solutions at the ratio of 9 : 1 and 3 : 7 (Fig. S3†). Although it was observed that the presence of PVA could affect the diameter of the nanofibers, this effect could not be quantified at this stage.

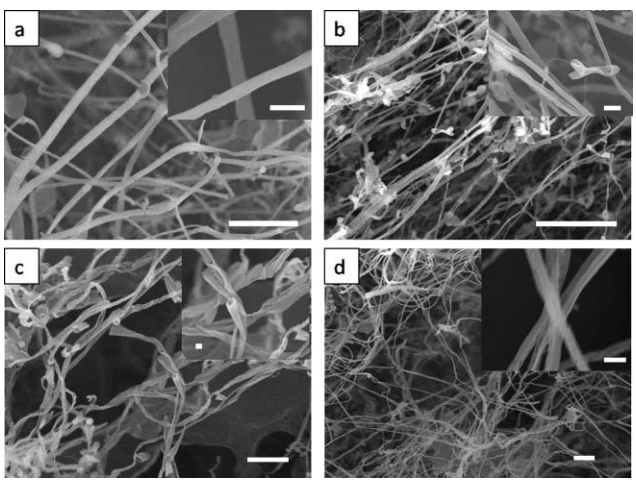

Fig. 2 Chitosan/PVA blend nanofibers prepared by freeze-drying the mixture of 0.1 wt% chitosan (MMw) and 0.1 wt% PVA aqueous solutions, volume ratio 7 : 3 (a); the same mixture at the volume ratio 5 : 5 (b); the mixture of 0.02 wt% chitosan (LMw)/0.02 wt% PVA, volume ratio 5 : 5 (c); the mixture 0.02 wt% chitosan (HMw)/0.02 wt% PVA, volume ratio 5 : 5 (d). All scale bars 10 μm, inset scale bars 1μm.

The chitosan (MMw) solution was replaced with chitosan (LMw) and chitosan (HMw) to investigate the formation of blend nanofibers. It was found that chitosan (HMw) could be used to form a nanofiber structure at a lower concentration such as 0.02 wt%. A mixture of 0.02 wt% chitosan (HMw) and 0.02 wt% PVA aqueous solutions at the volume ratio 5 : 5 was selected in this study. For comparison, the same concentration and volume ratio was used for chitosan (LMw). A kind of hollow fibrous structure was observed for the mixture of chitosan (LMw) and PVA (Fig. 2c). A cylindrical nanofiber structure with a diameter of around 500 nm was produced for the mixture of chitosan (HMw) and PVA (Fig. 2d). Although electrospinning was used to form chitosan/PVA blend nanofibers, only the use of chitosan solutions containing >50% PVA could produce smooth nanofibers. Beaded fibers were obtained for the solutions containing >50% chitosan.[8e] With our freeze-drying method, chitosan/PVA nanofibers with all the range of compositions could be produced.

3.3 Pore analysis and thermal stability of chitosan nanofibers

Pore size distribution and pore volume of chitosan structures were analyzed by mercury intrusion porosimetry. In order to see how the concentration could affect the porosity, chitosan materials were prepared by freeze-drying 0.1 wt%, 0.5 wt%, and 1.0 wt% aqueous chitosan solutions. Fig. 3 shows the pore size distribution and cumulative pore volumes of these chitosan materials. Chitosan materials from 0.1 wt% and 0.5 wt% solutions exhibited a similar pore size distribution with the peak located around pores at 180 μm, 60 μm, and a wide range of smaller pores (Fig. 3a). The pore size distribution for porous chitosan made from 1 wt% solution is slightly different, with the peaks around 180 μm and 20 μm. However, the pore volume of the porous chitosan materials increased consistently with the decrease of the chitosan concentration. As can be seen in Fig. 3b, chitosan nanofibers made from 0.1 wt% solution exhibited the highest pore volume of 33.32 ml g^{-1}, which was 1.5 and 2.4 times the pore volume of the chitosan materials prepared from 0.5 wt% (22.71 ml g^{-1}) and 1.0 wt% chitosan (13.89 ml g^{-1}) solutions. For the chitosan solution with a lower concentration, there was a larger portion of ice in the frozen sample. The removal of ice by freeze-drying would lead to a higher pore volume. The pore volume could directly affect the swelling behaviour of chitosan materials in water. It was found that chitosan nanofibers exhibited a fast adsorption activity in water and could reach equilibrium within 1 h. For the chitosan materials prepared from 0.5 wt% and 1.0 wt% solutions, it took about one day and seven days to reach the equilibrium adsorption.

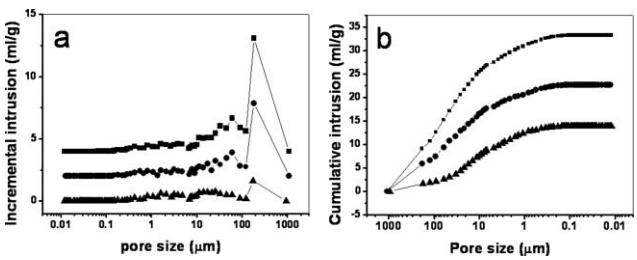

Fig. 3 Pore size distribution and cumulative intrusion volume of chitosan structures made from freeze -drying 0.1 wt% chitosan (MMw) (■), 0.5 wt% chitosan (MMw) (●) and 1.0 wt% chitosan (MMw) (▲) solutions, as characterized by mercury intrusion porosimetry. (a) Incremental intrusion volume *vs.* pore size. (b) Cumulative intrusion volume *vs.* pore size.

Thermal stability of chitosan and chitosan/PVA blend nanofibers was assessed by TGA analysis. The first-order derivative of thermogravimetric profiles (the rate of mass loss in relation to the temperature change) of chitosan (MMw) powder, pure chitosan (MMw) nanofibers, and 50% chitosan (MMw)/50% PVA are shown in Fig. 4. The decomposition temperature of chitosan powder was 307 °C. This could be attributed to the dehydration of the saccharide rings and the decomposition of the acetylated and deacetylated units of chitosan.[14a] For chitosan nanofibers, the decomposition temperature decreased to 282 °C. The reduction in decomposition temperature was likely due to the presence of a small amount of acetic acid which induced the thermal degradation compared to chitosan powders.[14b,14c] For chitosan/PVA nanofibers with the mass ratio 1 : 1, the decomposition temperature was reduced further to 266 °C although the PVA nanofibers prepared from 0.1 wt% aqueous PVA solution were decomposed at 293 °C. The blend nanofibers decomposed at a lower temperature than pure nanofibers. This indicated the possible formation of a less stable component in the blend nanofibers.

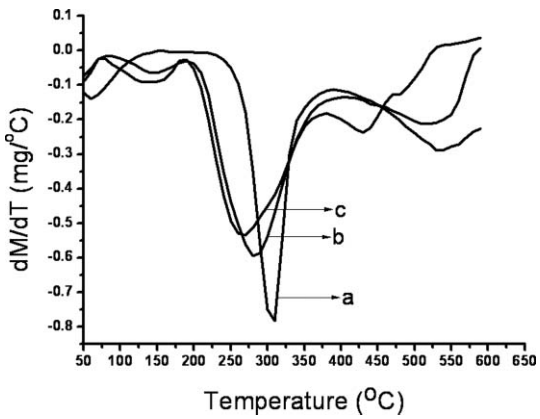

Fig. 4 First-order derivative of TGA curves of as-purchased chitosan powder (MMw) (a), chitosan nanofibers (MMw) made from 0.1 wt% aqueous solution (b), chitosan/PVA blend nanofibers prepared from the mixture of 0.1 wt% chitosan (MMw) solution and 0.1 wt% PVA solution at the volume ratio of 5 : 5 (c).

3.4 Biomineralization of chitosan nanofibers

A composite material of chitosan fibers and calcium phosphate is expected to increase the biocompatibility together with improved mechanical strength.[15] A porous biodegradable polymeric structure coated with hydroxyapatite is useful as a scaffold for bone tissue engineering and as a drug carrier for controlled release.[2,16] Biomimetic mineralization is a widely used route for the formation of calcium phosphate on polymer surfaces in the simulated body fluid (SBF).[17] Recently, the mineralization in 1.5 times[17b] and 10 times concentrated SBF[18] were carried out to form a calcium phosphate coating on polymer fibers, thus reducing the mineralization time significantly. The surface of the polymer fibers was modified before conducting mineralization in the SBF.[17,18] Here, we wanted to study whether chitosan nanofibers prepared by freeze-drying could be coated with calcium phosphate directly *via* the mineralization in the SBF.

The chitosan nanofibers prepared from 0.1 wt% aqueous solution were firstly immersed into the 10 times concentrated simulated body fluid (10-SBF) overnight. It was found that all the nanofibers were immobilized into thick calcium phosphate layers to form a strong hybrid material. The fibrous structure could no longer be observed. The 10-SBF solution was then replaced with a 5 times concentrated simulated body fluid (5-SBF) for the mineralization process. Fig. 5a shows the SEM image of chitosan (MMw) nanofibers after mineralization in 5-SBF for 6 h. 1.5 mg chitosan fibers were added into the 5-SBF. After mineralization, the mass of the material increased to 3.1 mg, a more than 100% mass gain. The chitosan nanofibers were coated with calcium phosphate and the nanofiber structure was still clearly observed. It was reported that nanohydroxyapatite could be formed on a chitosan-gelatin network *in situ*.[19] The amino and carbonyl groups of chitosan might be the active sites for nucleation, forming nuclei of nanohydroxyapatite. In this work, chitosan nanofibers could promote nucleation and growth of calcium phosphates, and resulted in a uniform mineralization layer on the nanofiber surface. The PXRD pattern confirmed that calcium phosphate mostly consisted of calcium pyrophosphate ($Ca_2P_2O_7$, labeled with *), by comparing with the standard pattern (JCPDS 23-0871) (Fig. 5b). $Ca_2P_2O_7$ may be used as nucleation sites for hydroxyapatite crystals in the bone structures for various applications.[19b,c] The PXRD pattern also shows the presence of another component $Ca_3(PO_4)_2{\cdot}xH_2O$. The EDX analysis showed the presence of calcium and phosphorous and a smaller percentage of potassium, sodium, and chlorine (Fig. S4†). The molar ratio of Ca/P was about 0.97, suggesting that the main component of the mineral layer was $Ca_2P_2O_7$.

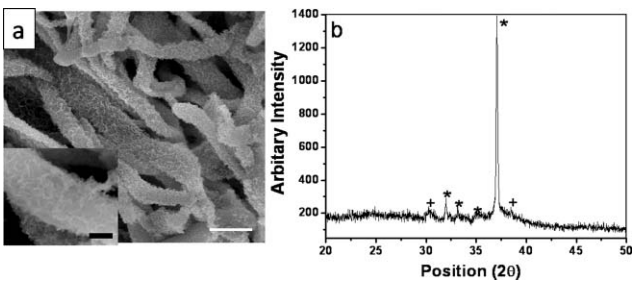

Fig. 5 a) SEM image of chitosan (MMw) nanofibers after mineralization process in 5-SBF for 6 h, scale bar 5 μm, inset scale bar 1 μm. b) The corresponding powder XRD pattern for the composite nanofibers. The peaks of $Ca_2P_2O_7$ and $Ca_3(PO_4)_2{\cdot}xH_2O$ are labeled with * and +, respectively.

3.5 Adsorption of Cu^{2+} for chitosan nanofibers in water

Chitosan can effectively adsorb metal ions due to the interaction of amine groups with metal ions and this property has been explored for waste water treatment.[3] Chitosan as an adsorbent for water treatment has many advantages including antimicrobial activity, biocompatibility, nontoxicity and low-cost, compared to the conventional methods such as chemical precipitation, reverse osmosis, electrodeposition, ion exchange, and evaporations.[20] Different chitosan materials including chitosan cross-linked with glutaraldehyde, chitosan flakes, and chitosan microspheres were utilized to adsorb metal ions.[3b,21] Recently, it was found that electrospun chitosan nanofibers

Table 1 The capacity and percentage of Cu^{2+} adsorption by chitosan nanofibers (4.0 mg) from aqueous $CuSO_4$ solutions (12.0 ml) with different concentrations

$CuSO_4$ solution (ppm)	50	100	200	400	600	1000
Adsorption amount (mmol copper/g chitosan)	0.35	0.67	1.00	1.54	2.06	2.57
Percentage of Cu^{2+} adsorbed (%)	37.3	35.7	26.7	20.53	18.3	13.7

could effectively adsorb Cu^{2+} in water and the adsorption capacity was improved compared with other types of chitosan materials.[3d] Here, chitosan nanofibers prepared by freeze-drying were assessed for the adsorption of Cu^{2+} from aqueous solutions. Aqueous $CuSO_4$ solutions with concentrations in the range of 50 to 1000 ppm were used to soak the chitosan nanofibers prepared from the 0.1 wt% aqueous chitosan (MMw) solution. It was found that the mass of the fibers increased gradually with time up until soaking for 8 h. After 8 h, there was no obvious mass change. The adsorption process continued for 16 h to make sure that adsorption saturation was reached in this study. The average adsorption amount increased from 0.35 to 2.57 mmol copper/g chitosan with the increase of the initial Cu^{2+} concentration in water while the percentage of Cu^{2+} adsorbed from the solutions decreased from 37.3% to 13.7% (Table 1). The percentage of Cu^{2+} removal from water was not particularly high. However, it should be noted that this study aimed to assess the adsorption capacity of chitosan nanofibers prepared by freeze-drying. The soaking condition including the mass of chitosan nanofibers and the volume of $CuSO_4$ solution was not optimized.

The adsorption of Cu^{2+} from $CuSO_4$ solutions was analysed by the Langmuir adsorption equation.[3d] The saturated adsorption capacity of chitosan nanofibers was calculated to be 3.85 mmol copper/g chitosan (246.91 mg copper/g chitosan), which was higher than that from electrospun chitosan nanofibers (2.85 mmol cooper/g chitosan)[3d] and chitosan microspheres (1.27 mmol or 80.71 mg cooper/g chitosan).[21a] When the chitosan material obtained from freeze-drying the 0.5 wt% solution was immersed in the 400 ppm $CuSO_4$ solution for 16 h, the average adsorption amount was 0.89 mmol copper/g chitosan, which was lower compared with that of chitosan nanofibers (average 1.54 mmol copper/g chitosan) under the same conditions. This indicated that chitosan nanofibers exhibited high adsorption capability for Cu^{2+}, likely resulting from high surface area, high porosity, and easily accessible active sites of the material.

3.6 Chitosan nanofibers as scaffolds for controlled release

Chitosan has been used for drug delivery due to its biocompatibility and non-toxicity. Porous chitosan, chitosan hydrogel, and chitosan microspheres were reported for drug and protein delivery.[22] Here, chitosan nanofibers as scaffolds for drug and protein delivery were examined. RhB and BSA were selected as the model compounds for this study. Chitosan nanofibers containing RhB or BSA were prepared by freeze-drying the 0.1 wt% chitosan solution containing RhB or BSA. As shown by the SEM images, the nanofiber structure was formed with the inclusion of RhB or BSA (Fig. 6). Different loading of RhB in chitosan nanofibers

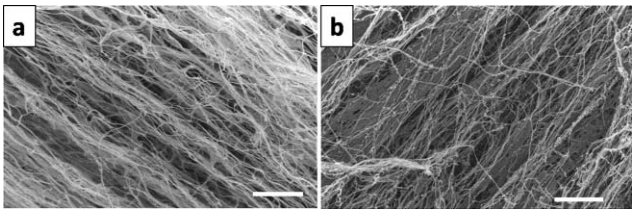

Fig. 6 SEM images of chitosan/RhB (a) and chitosan/BSA (b) nanofibers prepared by freeze-drying 0.36 μg RhB/ml 0.1 wt% chitosan and 1.0 mg BSA/ml 0.1 wt% chitosan. Scale bar 20 μm.

prepared from 0.1 wt% chitosan solution was firstly investigated. With high loading of RhB at 0.495 wt%, a fast release profile was observed (solid square in Fig. 7a). The released RhB reached a plateau after about 30 min. About 95% of loaded RhB was released at this stage. For the low loading of RhB at 0.036 wt%, the release of RhB into PBS was much slower (solid triangle in Fig. 7a). The release curve reached the plateau after 2 h. About 70% RhB was released in 200 min. Chitosan scaffolds prepared from different concentrations of chitosan solutions but with the same loading of RhB (0.036 wt%) were also employed for the RhB release into the PBS. Porous chitosan materials were prepared from 0.5 wt% and 1.0 wt% aqueous chitosan solutions with the same loading of RhB at 0.036 wt%. A slower release was observed for both scaffolds made from 0.5 wt% and 1.0 wt% chitosan solutions (solid circle and hollow square in Fig. 7a). Freeze-drying of 0.1 wt% chitosan solutions produced nanofibers. However, non-fiber porous structures were formed for the samples made from 0.5 wt% and 1.0 wt% chitosan solutions (Fig. S5†). The smaller pore volumes (see Fig. 3) for chitosan materials made from 0.5 wt% and 1.0 wt% led to slower soaking in aqueous solutions. More importantly, these non-fiber porous structures showed dense and thick chitosan walls and therefore lower surface areas for RhB release into water. This was demonstrated by the slower release of RhB from porous chitosan made at 0.5 wt% and 1.0 wt%. It should be noted that the morphology of chitosan structure was more important in affecting the release of RhB than the pore volume. In Fig. 7a, chitosan materials with the same loading of RhB but made from 0.5 wt% and 1.0 wt% exhibited different pore volumes but similar RhB release profiles. When chitosan nanofibers were made from 0.01 wt% aqueous solutions, these fibers exhibited

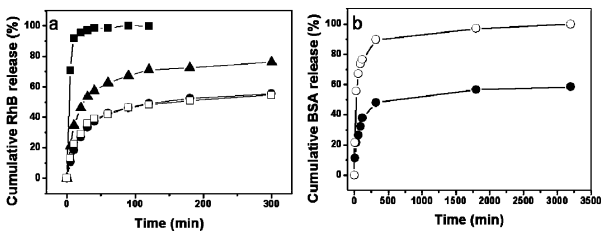

Fig. 7 (a) The release of RhB with time into the PBS from RhB-loaded chitosan structures prepared by freeze-drying the solutions of 4.95 μg RhB/ml 0.1 wt% chitosan (MMw) (■, 0.495 wt% loaded); 0.36 μg RhB/ml 0.1 wt% chitosan (▲, 0.036 wt% loaded); 1.80 μg RhB/ml 0.5 wt% chitosan solution (●, 0.036 wt% loaded); 3.60 μg RhB/ml 1.0 wt% chitosan solution (□, 0.036 wt% loaded). (b) The release of BSA with time into the PBS from BSA-loaded chitosan nanofibers prepared by freeze-drying 0.5 mg BSA/ml 0.1 wt% chitosan (●, 50 wt% loaded) and 1.0 mg BSA/ml 0.1 wt% chitosan (○, 100 wt% loaded).

higher permeability due to the large pore volume, the small diameters of chitosan fibers (high surface area), and the fast swelling activity. The buffer solution could be easily penetrated into the fibrous structure. A fast release of RhB molecules into the buffer solution was observed (Fig. 7a).

Compared with RhB, BSA was released slowly from the chitosan nanofibers even at a much higher loading, primarily due to the large molecular size (Fig. 7b). The initial release of BSA was relatively fast and about 40% of loaded BSA was released in 200 min when the loading of BSA in chitosan nanofibers was 50 wt%. After 200 min, the release became slower and about 60% of loaded BSA was released after 50 h. When the loading of BSA was doubled (100 wt% loading, the curve labelled with hollow circle in Fig. 7b), the release profile was similar, *i.e.*, a fast initial release of 80% of loaded BSA until 200 min followed by a reducing release rate. However, a higher percentage of BSA was released from the nanofibers when the loading was increased. Because chitosan is insoluble in PBS, the release was dependent on the diffusion of BSA from the nanofiber scaffold. The BSA on or close to the nanofiber surfaces could be rapidly diffused out into the PBS. When the loading of BSA was increased, the amount of BSA on or close to the nanofiber surface was increased accordingly. This could explain the higher percentage release of BSA from chitosan nanofibers when the loading was doubled. After the initial fast release, BSA was slowly diffused out of the nanofibers due to the hydrogen-bonding interaction with chitosan chains.[22c]

4. Conclusions

In summary, we demonstrated a simple and green method for the preparation of chitosan nanofibers by freeze-drying diluted aqueous solutions. Chitosan nanofibers with diameters in the range of 100 to 700 nm were produced. The low concentration of aqueous solution and low freezing temperature were critical for the formation of nanofibers. Chitosan nanofibers with low, medium, and high molecular weights were produced, but with a lower concentration required for the chitosan with high molecular weight. Chitosan/PVA blend nanofibers with different mass ratios were also produced using this method. Pore size distribution and pore volume, thermal stability, and swelling property of the chitosan nanofibers were investigated. A calcium phosphate layer mainly composed of $Ca_2P_2O_7$ was formed onto the chitosan nanofiber surface *via* a mineralization process in a 5 times concentrated simulated body fluid. The chitosan nanofibers were used to adsorb Cu^{2+} ions in water and exhibited a higher adsorption capacity than that of electrospun chitosan nanofibers and chitosan microspheres. RhB and BSA loaded chitosan nanofibers were prepared and their release into the PBS was studied. The small RhB molecules were released faster from the nanofibers than the large BSA molecules. It was also found that RhB was released faster from the nanofibers than from porous chitosan.

Acknowledgements

This work was supported by the EPSRC (EP/F016883/1). HZ is a RCUK Academic Fellow. We acknowledge the Center for Materials Discovery at Liverpool for access to the SEM and TGA.

References

1 (*a*) M. N. V. R. Kumar, *React. Funct. Polym.*, 2000, **46**, 1–27; (*b*) E. Khor and L. Y. Lim, *Biomaterials*, 2003, **24**, 2339–2349; (*c*) H. K. No, N. Y. Park, S. H. Lee and S. P. Meyers, *Int. J. Food Microbiol.*, 2002, **74**, 65–72; (*d*) H. Ueno, T. Mori and T. Fujinaga, *Adv. Drug Delivery Rev.*, 2001, **52**, 105–115; (*e*) N. Angelova, I. Rashkov, V. Maximova, S. Bogdanova and A. Domard, *J. Bioact. Compat. Polym.*, 1995, **10**, 285–98; (*f*) E. R. Selmer-Olsen, H. C. Ratnaweera and R. Pehrson, *Water Sci. Technol.*, 1996, **34**, 33–40.

2 (*a*) J. Berger, M. Reist, J. M. Mayer, O. Felt and R. Gurny, *Eur. J. Pharm. Biopharm.*, 2004, **57**, 35–52; (*b*) Y. J. Park, Y. M. Lee, S, N. Park, S. Y. Sheen, C. P. Chung and S. J. Lee, *Biomaterials*, 2000, **21**, 153–159; (*c*) Y. Zhang and M. Q. Zhang, *J. Biomed. Mater. Res.*, 2002, **62**, 378–386; (*d*) S. Haider, S. Y. Park and S. H. Lee, *Soft Matter*, 2008, **4**, 485–492; (*e*) K. Desai, K. Kit, J. J. Li and S. Zivanovic, *Biomacromolecules*, 2008, **9**, 1000–1006; (*f*) H. Z. Huang and X. R. Yang, *Biomacromolecules*, 2004, **5**, 2340–2346; (*g*) L. Qian and X. R. Yang, *Talanta*, 2006, **68**, 721–727.

3 (*a*) Y. Qin, H. Hu, A. Luo, Y. Wang, X. Huang and P. Song, *J. Appl. Polym. Sci.*, 2006, **99**, 3110–3115; (*b*) W. S. Wan Ngah, C. S. Endud and R. Mayanar, *React. Funct. Polym.*, 2002, **50**, 181–190; (*c*) W. Kaminski, E. Tomczak and K. Jaros, K., *Desalination*, 2008, **218**, 281–286; (*d*) S. Haider and S.-Y. Park, *J. Membr. Sci.*, 2009, **328**, 90–96.

4 N. Bhattaraia, D. Edmondsona, O. Veiseha, F. A. Matsenb and M. Zhang, *Biomaterials*, 2005, **26**, 6176–6184.

5 (*a*) D. Li and Y. Xia, *Adv. Mater.*, 2004, **16**, 1151–1170; (*b*) D. H. Reneker, A. L. Yarin, H. Fong and S. Koombhongse, *J. Appl. Phys.*, 2000, **87**, 4531–4547; (*c*) D. H. Reneker and I. Chun, I., *Nanotechnology*, 1996, **7**, 216–223; (*d*) R. M. Capito, H. S. Azevedo, Y. S. Velichko, A. Mata and S. I. Stupp, *Science*, 2008, **319**, 1812–1816; (*e*) V. J. Chen, A. L. Smith and P. X. Ma, *Biomaterials*, 2006, **27**, 3973–3979.

6 (*a*) N. Bhattarai, Z. Li, J. Gunn, M. Leung, A. Cooper, D. Edmondson, O. Veiseh, M.-H. Chen, Y. Zhang, R. G. Ellenbogen and M. Zhang, *Adv. Mater.*, 2009, **21**, 2792–2797; (*b*) M. G. McKee, J. M. Layman, M. P. Cashion and T. E. Long, *Science*, 2006, **311**, 353–355; (*c*) M. P. Lutolf and J. A. Hubbell, *Nat. Biotechnol.*, 2005, **23**, 47–55.

7 (*a*) R. R. Klossner, H. A. Queen, A. J. Coughlin and W. E. Krause, *Biomacromolecules*, 2008, **9**, 2947–2953; (*b*) L. Li and Y. L. Hsieh, *Carbohydr. Res.*, 2006, **341**, 374–381; (*c*) M. G. McKee, G. L. Wilkes, R. H. Colby and T. E. Long, *Macromolecules*, 2004, **37**, 1760–1767.

8 (*a*) Y. Zhou, D. Yang, X. Chen, Q. Xu, F. Lu and J. Nie, *Biomacromolecules*, 2008, **9**, 349–354; (*b*) Y. T. Jia, J. Gong, X. H. Gu, H. Y. Kim and J. Dong, *Carbohydr. Polym.*, 2007, **67**, 403–409; (*c*) Y. S. Zhou, D. Z. Yang and J. J. Nie, *J. Appl. Polym. Sci.*, 2006, **102**, 5692–5697; (*d*) W. H. Park, L. Jeong, D. Yoo and S. Hudson, *Polymer*, 2004, **45**, 7151–7157; (*e*) K. Ohkawa, D. Cha, H. Kim, A. Nishida and H. Yamamoto, *Macromol. Rapid Commun.*, 2004, **25**, 1600–1605; (*f*) D. S. Jessica and L. S. Caroline, *Biomacromolecules*, 2007, **8**, 594–601; (*g*) B.-M. Min, S. W. Lee, J. N. Lim, Y. You, T. S. Lee, P. H. Kang and W. H. Park, *Polymer*, 2004, **45**, 7137–7142; (*h*) X. Y. Geng, O.-H. Kwon and J. H. Jiang, *Biomaterials*, 2005, **26**, 5427–5432; (*i*) H. Homayoni, S. A. H. Ravandi and M. Valizadeh, *Carbohydr. Polym.*, 2009, **77**, 656–661.

9 M. C. Gutiérrez, M. L. Ferrer and F. del Monte, *Chem. Mater.*, 2008, **20**, 634–648.

10 L. Qian, E. Willneff and H. F. Zhang, *Chem. Commun.*, 2009, 3946–3948.

11 A. C. Tas and S. B. Bhaduri, *J. Mater. Res.*, 2004, **19**, 2742–2749.

12 H. Zhang, I. Hussain, M. Brust, M. F. Butler, S. R. Rannard and A. I. Cooper, A. I., *Nat. Mater.*, 2005, **4**, 787–793.

13 J. Gong, X. Hu, K. Wong, Z. Zheng, L. Yang, W. Lau and R. Du, *Adv. Mater.*, 2008, **20**, 2111–2115.

14 (*a*) C.-H. Chen, F.-Y. Wang, C.-F. Mao and C.-H. Yang, *J. Appl. Polym. Sci.*, 2007, **105**, 1086–1092; (*b*) L. Qi, S. Pal, P. Dutta, M. Seehra and M. Pei, *J. Biomed. Mater. Res., Part A*, 2008, **87a**, 236–244; (*c*) J. M. Yang, W. Y. Su, T. L. Leu and M. C. Yang, *J. Membr. Sci.*, 2004, **236**, 39–51.

15 (*a*) T. Yoshioka, H. Onomoto, H. Kashiwazaki, N. Inoue, Y. Koyama, K. Takakuda and J. Tanaka, *Mater. Trans.*, 2009, **50**, 1269–1272; (*b*) A. Matsuda, T. Ikoma, H. Kobayashi and J. Tanaka, *Mater. Sci. Eng., C*, 2004, **24**, 723–728.

16 A. Oyanea, M. Uchidab, C. Choongc, J. Triffittc, J. Jonesd and A. Ito, *Biomaterials*, 2005, **26**, 2407–2413.
17 (*a*) A. Oyane, M. Uchida, Y. Yokoyama, C. Choong, J. Triffitt and A. Ito, *J. Biomed. Mater. Res., Part A*, 2005, **75a**, 138–145; (*b*) X. Y. Yuan, A. F. T. Mark and J. L. Li, *J. Biomed. Mater. Res.*, 2001, **57**, 140–150.
18 X. R. Li, J. W. Xie, X. Y. Yuan and Y. N. Xia, *Langmuir*, 2008, **24**, 14145–14150.
19 (*a*) J. J. Li, Y. P. Chen, Y. J. Yin, F. L. Yao and K. D. Yao, *Biomaterials*, 2007, **28**, 781–790; (*b*) J. Sun, Y. Tsung, C. Liao, H. Liu, Y. Hang and F. Lin, *J. Biomed. Mater. Res.*, 1997, **37**, 324–334; (*c*) S. O. Rogero, F. J. C. Braga and O. Z. Higa, *Mater. Sci. Forum*, 1999, **299–300**, 44–47.
20 (*a*) J. C. Y. Ng, W. H. Cheung and G. Mckay, *J. Colloid Interface Sci.*, 2002, **255**, 64–74; (*b*) K. C. Justi, V. T. Făıvere, M. C. M. Laranjeira, A. Neves and R. A. Peralta, *J. Colloid Interface Sci.*, 2005, **291**, 369–374.
21 R. Bassi, S. O. Prasher and B. K. Sampson, *Sep. Sci. Technol.*, 2000, **35**, 547–560.
22 (*a*) M. Temtem, M. C. Silva, P. Z. Andrade, F. Santos, C. L. da Silva, J. M. S. Cabral, M. M. Abecasis and A. Aguiar-Ricardo, *J. Supercrit. Fluids*, 2009, **48**, 269–277; (*b*) F.-L. Mi, S.-S. Shyu, C.-T. Chen and J.-Y. Schoung, *Biomaterials*, 1999, **20**, 1603–1612; (*c*) Z. M. Wu, X. G. Zhang, C. Zheng, C. X. Li, S. M. Zhang, R. N. Dong and D. M. Yu, *Eur. J. Pharm. Sci.*, 2009, **37**, 198–206.

